

CrystEngComm

Accepted Manuscript



This is an *Accepted Manuscript*, which has been through the Royal Society of Chemistry peer review process and has been accepted for publication.

Accepted Manuscripts are published online shortly after acceptance, before technical editing, formatting and proof reading. Using this free service, authors can make their results available to the community, in citable form, before we publish the edited article. We will replace this *Accepted Manuscript* with the edited and formatted *Advance Article* as soon as it is available.

You can find more information about *Accepted Manuscripts* in the [Information for Authors](#).

Please note that technical editing may introduce minor changes to the text and/or graphics, which may alter content. The journal's standard [Terms & Conditions](#) and the [Ethical guidelines](#) still apply. In no event shall the Royal Society of Chemistry be held responsible for any errors or omissions in this *Accepted Manuscript* or any consequences arising from the use of any information it contains.

A two-dimensional Cu^{II}-Mn^{II} heterometallic coordination polymer: structure determination using synchrotron X-ray powder diffraction and magnetic properties

Marguerite Kalisz^{†,‡}, Rafael A. A. Cassaro^{‡,†}, Miguel A. Novak[#], Marius Andruh[§],
Helio S. Amorim^{#*}, Maria G. F. Vaz^{†*}

[†] Universidade Federal Fluminense, Instituto de Química, Niterói, Rio de Janeiro, Brazil.

[‡] Universidade Federal do Rio de Janeiro, Instituto de Química, Rio de Janeiro, Brazil.

[#] Universidade Federal do Rio de Janeiro, Instituto de Física, Rio de Janeiro, Brazil.

[§] Inorganic Chemistry Laboratory, Faculty of Chemistry, University of Bucharest, Str. Dumbrava Rosie nr. 23, 020464-Bucharest, Romania.

ABSTRACT

In this work we describe the structure of a coordination polymer which was solved by using synchrotron X-ray powder diffraction. The heterometallic Cu^{II}-Mn^{II} compound [Cu₂Mn₂(bopba)(DMSO)₇].DMSO, was assembled from a binuclear oxamato copper(II) complex and manganese(II) ions, generating a Mn-Cu-Mn-Cu-chain motif. Each chain is connected to two others, resulting in a folded two-dimensional coordination network where the uncoordinated DMSO molecule is located in the space between the layers. The loss of the DMSO molecules leads to a loss of both crystallinity and long range magnetic order. The knowledge of the structure allowed quantifying the intrachain magnetic interaction.

INTRODUCTION

The main interest in heterometallic complexes containing paramagnetic ions arises from their magnetic properties¹. The ideal case, when designing magnetic materials is to assemble within the same molecular entity metal ions that are ferromagnetically coupled. However, strict orthogonality of magnetic orbitals, which affords a ferromagnetic interaction, can be achieved only for a few pairs of metal ions². An alternative strategy is to combine a metal ion with a large spin quantum

number with another one having a small one. Consequently, even if the exchange interaction between the metal centers is antiferromagnetic, the ground state will be ferrimagnetic. This was the original strategy developed by Kahn and his school to obtain molecular magnets³⁻⁴. For example, one of the first rationally designed molecular materials showing spontaneous magnetization below a critical temperature was synthesized employing Mn^{II} ($S = 5/2$) and Cu^{II} ($S = 1/2$) ions.⁵ The most important conditions to be fulfilled by a synthetic strategy leading to such systems are: (i) have good control over the structural topology of the spin carriers; (ii) achieve a strong exchange interaction between the metal ions, mediated by bridging ligands. The first condition can be achieved using metalloligands as building blocks, which are generally anionic complexes containing potentially bridging ligands. The number and the geometrical disposition of these ligands -- as well as the charge of the metalloligand -- play a crucial role in directing the self-assembly processes. Other important factors are: the stereochemical preference of the assembling cations, their charge, and the presence/absence of blocking ligands.

Classical metalloligands, widely employed to construct magnetic coordination polymers, are: homoleptic and heteroleptic cyanido complexes;⁶⁻¹² homoleptic and heteroleptic oxalato complexes;¹³⁻²⁰ isothiocyanato complexes;²¹ bis-oxamato-complexes.²² Let us briefly refer to this last family of metalloligands since they are related to the present work. The general structure of archetypal bis-oxamato copper(II) complexes is presented in Chart 1a. The self-assembly processes involving these anionic species with various transition metal cations (Mn^{II}, Co^{II}, Ln^{III}) afforded coordination polymers with beautiful topologies and exciting magnetic properties.²³⁻²⁹ More recently, the library of oxamato copper(II) building-blocks was enriched with new members obtained using more sophisticated oxamato ligands. Among these we recall bis(bidentate) oxamates that generate binuclear copper(II) metalloligands (Chart 1 - b,c), and oxamato ligands functionalized with additional groups (Chart 1 - d-f) that bring additional new properties (chirality, photo- or redox activity) that can lead to *multifunctional* magnetic materials^{22,30-31}

In all these cases the magnetic properties are deeply linked to the arrangement of the magnetic moment carriers in the crystalline network. Therefore, the correlation between crystalline structure and magnetic properties, referred to magnetostructural analysis, has been used to understand the magnetic behavior of molecular magnetic compounds. Since magnetic interactions depend strongly on distance and angles

between magnetic moments carriers, knowledge of the crystalline structure is a quasi-unavoidable information to understand magnetic properties and analyze them quantitatively. However, there are circumstances where growing suitable single crystals is not feasible. In some such cases, crystal structures have been determined using powder X-ray diffraction.³² Structure determination from powder diffraction can be significantly more laborious than from single crystal X-ray diffraction data, and the accuracy obtained for bond lengths, bond angles and torsion angles is often lower. Use of synchrotron radiation is very helpful to prevent multiple Bragg peaks from overlapping in a powder pattern, allowing each peak to be independently measured. A combination of complementary information about chemical composition, NMR, IR absorption spectroscopy, powder densitometry, thermogravimetric analysis, and any prior information about the molecular structure of initial building blocks can be combined with powder diffraction as a reliable strategy to determine crystal structures without having a single crystal.

In this paper we report a new 2-D coordination polymer, the bimetallic Cu^{II}-Mn^{II} compound $[\text{Cu}_2\text{Mn}_2(\text{bopba})(\text{DMSO})_7]\cdot\text{DMSO}$ (**1a**) (DMSO = dimethylsulfoxide), that was assembled from a binuclear oxamato copper(II) complex and manganese(II) ions. The structure of the metalloligand³³ $[\text{Cu}_2(\text{bopba})]^{4-}$ is given in Chart 1g [bopba = bis-(o-phenylene-bis(oxamate))]. In spite of all efforts, we were not able to obtain single crystals for X-ray diffraction. However, by combining other techniques with high intensity synchrotron X-ray powder diffraction, we were able to determine a structural model for this compound. As a result, the magnetic properties could be quantitatively investigated, allowing us to identify the effect of entrained solvent molecules on the magnetic behavior.

Chart 1

RESULTS AND DISCUSSION

The targeted bimetallic Cu^{II}-Mn^{II} compound was obtained by self-assembly of $[\text{Cu}_2(\text{bopba})]^{4-}$ tectons with manganese(II) ions. The particular structure of the binuclear building block -- with two copper-bis(oxamato) groups making a 60° angle with respect to the bis-phenylene organic spacer connecting them -- suggests

interesting topologies of the resulting bimetallic coordination polymers. The infrared spectrum of the product bimetallic complex confirms the coordination of the oxamato group to the manganese(II) ion: the $\nu(\text{C}=\text{O})$ band of the precursor³³, $(\text{NBu}_4)_4[\text{Cu}_2(\text{bopba})]$, is displaced to lower energy, from 1675 to 1595 cm^{-1} . The thermogravimetric analysis of **1a** between 20-1200 °C shows a loss of mass in the temperature range 20-350 °C, that can be associated with the loss of six DMSO molecules. Above 350 °C, the loss of mass is attributed to the loss of other DMSO molecules followed by ligand decomposition.

Structure

Powder X-ray diffraction data obtained for the bimetallic $\text{Cu}^{\text{II}}\text{-Mn}^{\text{II}}$ compound (**1a**) was indexed to identify a primitive monoclinic cell: $a = 16.92 \text{ \AA}$, $b = 9.13 \text{ \AA}$, $c = 18.19 \text{ \AA}$ and $\beta = 92.9^\circ$ ($V = 2807 \text{ \AA}^3$). On the basis of systematic absences and by comparing the calculated and obtained powder density, the space group was initially assigned as Pc with two molecules per unit cell ($Z = 2$). During the course of structure resolution, it became clear that the manganese(II) cations are coordinated to the oxygen atoms in the oxamato groups of the $[\text{Cu}_2(\text{bopba})]$ fragment. The Mn–O bond length was assumed to be $\sim 2.15 \text{ \AA}$, similar to those reported for $\text{MnCu}(\text{opba})(\text{H}_2\text{O})_2\cdot\text{DMSO}$ ³⁴. Despite much effort from this assumption gave results that were unsatisfactory (the Reitveld refinement gives poor fits to the experimental powder XRD data -- $R_{\text{wp}}(\%) = 24.5$ and $\chi^2 = 7.42$) and yielded substantial void space that could not be reconciled with use of an appropriate number of DMSO molecules in the lattice. So, based on systematic absences in hkl , the space group was reassigned as $P2_1/c$. In order to retain the number of molecules per unit cell ($Z = 2$), in agreement with the expected powder density, the inversion center of the fragment $[\text{Mn}_2\text{Cu}_2(\text{bopba})]$, located in the middle of C-C bond that connects two phenyl rings (chart 1g), was fixed at the crystallographic inversion center (Wyckoff d site; $\frac{1}{2}, 0, \frac{1}{2}$). Only half of the fragment was considered in the asymmetric unit ($Z' = \frac{1}{2}$), so the inversion symmetry operation generates the complete molecule.

Figure 1

A structure determination by the simulated annealing (SA) method requires definition of molecular fragments in a unit cell. The $[\text{Cu}_2(\text{bopba})]^{4-}$ building block was presumed from the structure of $(\text{NBu}_4)_4[\text{Cu}_2(\text{bopba})]$, previously determined from single crystal measurements.³³ For the DMSO molecule, a rigid model was used with standard bond angles and bond lengths. The asymmetric unit considered was the $[\text{MnCu}(\text{bopba})]$ fragment and four DMSO molecules. The fragment was allowed only to have rigid rotation around the inversion center, while the DMSO molecules were allowed to translate and rotate freely, leading to 27 structural variables (3 rotational variables for the $[\text{MnCu}(\text{bopba})]$ and 6 for each DMSO molecule).

Furthermore, the number of DMSO molecules per unit cell in $P2_1/c$ is 16 (larger than the unrealistic number obtained using the Pc space group) and fulfills the need for an appropriate number solvate molecules in the structure. After many runs of Monte Carlo steps calculation, a structure solution was obtained, and then used as the starting structural model for Rietveld refinement. A routine for crystal structure refinements based on rigid-body model with constrained generalized coordinates and mean thermal displacements assuming the same isotropic displacement parameter (B_{iso}) for all atoms, was applied as implemented in the Fullprof program. Hydrogen atoms were included in the later stages of simulation, using conventional geometric restraints on their bond lengths and bond angles. These restraints were gradually relaxed for the final refinement. We next considered five independently isotropic displacements for the four DMSO molecules and for the $[\text{MnCu}(\text{bopba})]$ fragment. The B_{iso} for all DMSO molecules were larger than the values found for the $[\text{MnCu}(\text{bopba})]$ fragment, indicating that the DMSO molecules are disordered. We tried to model these disordered solvent molecules by splitting them into two categories, but this strategy was unsuccessful. However, the lack of precise placements for the DMSO molecules did not prevent confident identification of the main coordination structure.

Figure 2

Table 1

Figure 2

Based on the above results, we were now able to describe the structure of compound **1a**. The copper(II) ions within the bis-oxamato moieties have a pentacoordinated, distorted square-pyramidal geometry, in which two oxygen and two

nitrogen atoms from the oxamato group form the basal plane, and a DMSO molecule coordinated at the apical position). The manganese(II) ions are hexacoordinated by four oxygen atoms from two chelating oxamato groups of two $\{\text{Cu}_2(\text{bopba})\}$ units, plus two oxygen atoms from two DMSO molecules (Figure 2). As expected, each bis-oxamato end of the binuclear tecton coordinates to two manganese ions, generating a Mn-Cu-Mn-Cu- chain motif where the shortest $\text{Cu1}\cdots\text{Mn1}$ distance is ≈ 5.4 Å. This distance is similar to that found in the first oxamato bridged copper(II)-manganese(II) complexes described by Kahn et al.³⁵ Each chain is connected to two others, resulting in a layered, folded, two-dimensional coordination network, with 10-nodal meshes, where the nodes consist of copper and manganese ions (Figure 3). The intramolecular $\text{Cu1}\cdots\text{Cu1}$, $\text{Mn1}\cdots\text{Mn1}$ and $\text{Cu1}\cdots\text{Mn1}$ distances between adjacent chains are approximately 11.8 Å (1-*x*, -*y*, 1-*z*), 10.8 Å (1-*x*, -0.5+*y*, 1.5-*z*) and 11.4 Å (1-*x*, -0.5+*y*, 1.5-*z*), respectively. A view along the crystallographic *a*-axis is shown in Figure 4.

Figure 3

Figure 4

The layers formed by these units are disposed parallel to each other at distance of ~ 3.8 Å (Figure 5), where the shortest distance between paramagnetic centers ($\text{Cu1}\cdots\text{Cu1}$) 2-*x*, 1-*y*, 1-*z*) in adjacent layers is ≈ 7.4 Å. The uncoordinated DMSO molecules reside in the space between the layers. All DMSO molecules show some level of disorder. Although it was not possible to determine accurately the position and orientation of lattice DMSO molecules, it is clear that these solvent molecules are strongly linked to the stability of the structure, since their loss under vacuum at room temperature leads to collapse of the crystal structure integrity (see below).

Figure 5

Magnetic properties

The bimetallic $\text{Cu}^{\text{II}}\text{-Mn}^{\text{II}}$ compound can be obtained with different entrained solvent quantities depending on the drying time under vacuum. In an extreme case, after one week under vacuum at room temperature, structure **1a** transforms into a nearly amorphous sample **1b**. The magnetic properties of **1a** were investigated between 2.5 and 291 K, and temperature dependence of the $\chi_{\text{M}}T$ is shown in Figure 6. At 291 K, $\chi_{\text{M}}T = 8.9 \text{ cm}^3\text{mol}^{-1}\text{K}$, smaller than that expected ($9.5 \text{ cm}^3\text{mol}^{-1}\text{K}$) for the

four uncoupled metal ions (2Cu^{II} and 2Mn^{II}). From the determined structure, the strongest exchange interaction is expected to be antiferromagnetic, and to occur through the oxamato-bridged copper(II) and manganese(II) ions. Consequently, each chain within a layer would show ferrimagnetic behavior.² Indeed, by lowering the temperature, $\chi_{\text{M}}T$ decreases very slowly, reaching a minimum of $8.2 \text{ cm}^3\text{mol}^{-1}\text{K}$ at 110 K, then increases to a maximum of $47.8 \text{ cm}^3\text{mol}^{-1}\text{K}$ at 7.2 K. Below this temperature, $\chi_{\text{M}}T$ decreases to $36.2 \text{ cm}^3\text{mol}^{-1}\text{K}$ at 2.6 K.

In order to estimate the magnetic exchange coupling constant, the $\chi_{\text{M}}T$ versus T data were fitted using Seiden's ferrimagnetic chain model³⁶ given in Eq. 1. Here, the $S_{\text{Cu}} = 1/2$ spin units are treated as quantum spins, and the $S_{\text{Mn}} = 5/2$ are treated classically. Since the effects of weak interchain magnetic interactions are more relevant at low temperatures leading to long range magnetic ordering,³⁷ the data were fitted for $T > 70$ K. The molecular formula contains two ($\text{Mn}^{\text{II}}-\text{Cu}^{\text{II}}$) spin units, so the Seiden equation was multiplied by 2 to represent the calculated magnetic data for 1 mol of **1a**.

Figure 6

$$\begin{aligned}
 H &= -J \sum S_i \cdot S_{i+1} \\
 \chi T &= 2 \frac{N\mu_B^2}{3k} \left\{ g_{\text{Mn}}^2 S_{\text{Mn}}^2 \left(\frac{S_{\text{Mn}} + 1}{S_{\text{Mn}}} + \frac{2\delta}{1-\delta} \right) - 4g_{\text{Mn}}g_{\text{Cu}}\Lambda S_{\text{Cu}}S_{\text{Mn}} \frac{1}{1-\delta} + g_{\text{Cu}}^2 \left(S_{\text{Cu}}(S_{\text{Cu}} + 1) + 2\Lambda^2 S_{\text{Cu}}^2 \frac{1}{1-\delta} \right) \right\} \\
 \gamma &= -JS_{\text{Mn}} / kT \\
 a_0 &= 4(\gamma^{-1} \sinh \gamma - \gamma^{-2} \cosh \gamma + \gamma^{-2}) \\
 a_1 &= 12 \left[(\gamma^{-1} + 12\gamma^{-3}) \sinh \gamma - (5\gamma^{-2} + 12\gamma^{-4}) \cosh \gamma - \gamma^{-2} + 12\gamma^{-4} \right] \\
 b_0 &= \gamma^{-1} (\cosh \gamma - 1) \\
 b_1 &= 3 \left[(\gamma^{-1} + 4\gamma^{-3}) \cosh \gamma - 4\gamma^{-2} \sinh \gamma + \gamma^{-1} - 4\gamma^{-3} \right] \\
 \delta &= \frac{a_1}{3a_0}, \Lambda = 2 \left(\frac{b_1}{3a_0} + \frac{b_0}{a_0} \right)
 \end{aligned}
 \tag{Eq. 1}$$

The best fit curve (solid black line in Fig. 6) was found for $J = -39 \text{ cm}^{-1}$, $g_{\text{Cu}} = 2.40$ and $g_{\text{Mn}} = 2.02$. Although the g_{Cu} is moderately larger than typically found for copper(II) complexes, the magnetic coupling constant is in good agreement with values reported for oxamate $\text{Mn}^{\text{II}}-\text{Cu}^{\text{II}}$ coupled chains.^{4, 34, 38}

As described before, the space between the layers contains both coordinated and uncoordinated DMSO solvent molecules. Since the solvent may have an

important influence in the magnetic properties³⁹, we investigated this by comparing the magnetic responses of **1a** and **1b** (dried from **1a**). The desolvation process occurs without heating at room temperature, so covalent bonds between metal ions and the bopba ligand are not expected to break during desolvation, and the bidimensional magnetically relevant skeleton of the compound should be retained. The temperature dependence of $\chi_M T$ versus T in the range 2 – 35 K for the two samples is shown in Figure 7. Above 12 K, both samples present the same magnetic behavior. However, below this temperature, **1b** exhibits a loss of magnetic susceptibility. This suggests that the loss of solvent molecules leads to a loss of long range order, both crystalline and magnetic.

Figure 7

EXPERIMENTAL

All chemicals were purchased from Fluka and Aldrich, and were used without further purification. Elemental analysis was performed using a Perkin Elmer 2400. The metal analyses were carried out using an Agilent 4200 MP-AES. Infrared (IR) spectra were recorded with a Nicolet Magna 760 FT-IR spectrophotometer using samples in KBr pellets. Thermogravimetric analysis was performed using a Mettler Toledo TGA-DTA SDTA851 analyzer.

Synthesis

$[\text{Cu}_2\text{Mn}_2(\text{bopba})(\text{DMSO})_7] \cdot 2(\text{DMSO})$ was prepared by mixing a solution of $(\text{NBu}_4)_4[\text{Cu}_2(\text{bopba})]$ (synthesized as previously described³³) in DMSO with a solution of anhydrous manganese chloride in DMSO, as described in the literature.³⁷ After one hour, a green polycrystalline product was collected by filtration. Anal. Calc. for $\text{C}_{38}\text{H}_{60}\text{N}_4\text{O}_{21}\text{S}_9\text{Cu}_2\text{Mn}_2$: C, 31.81; H, 4.21; N, 3.90; Cu, 8.86; Mn, 7.65%. Found: C, 31.12; H, 4.31; N, 4.08; Cu, 8.70; Mn, 7.99%. IR spectroscopy: 1595 cm^{-1} : $\nu(\text{C}=\text{O})$. Compound **1a** was obtained by drying $[\text{Cu}_2\text{Mn}_2(\text{bopba})(\text{DMSO})_7] \cdot 2(\text{DMSO})$ for 2 hours under vacuum at room temperature. Sample **1b** was obtained after drying **1a** for one week under vacuum at room temperature.

Crystallography

X-ray diffraction data collection of (**1a**) polycrystalline sample was performed on the XPD (X-ray Powder Diffraction) D10B beam line at the Brazilian Synchrotron Light Laboratory (LNLS). A Huber 4+2 circles diffractometer, equipped with an Eulerian cradle, was used to perform the experiments in reflection $\theta - 2\theta$ geometry, with steps $2\theta = 0.03^\circ$ and wavelength 1.7711 Å. The diffractogram (Figure 1) was indexed with the TAUPIN⁴⁰ and DICVOL⁴¹ programs. Using the twenty first lines of the diffractogram, a primitive monoclinic cell was obtained with a high de Wolff figure of merit (M_{20}).⁴² The unit cell parameters were obtained refining the cell parameters by Le Bail method⁴³ and considering the whole diffractogram.

The crystal structure was determined by Simulated Annealing (SA) method⁴⁴⁻⁴⁵ such as implemented in the FOX⁴⁶ and DASH⁴⁷ programs. The structure models outlined in the simulated annealing step were refined by Rietveld method, using rigid body constraints, by a routine implemented in DASH and Fullprof. In addition, light effects of texture observed in the (flat) samples were adequately treated with the March-Dollase function. The Le Bail analyses were performed with the Fullprof program.⁴⁸ Summary of crystal data and structure refinement for **1a** are shown in Table 1 and Figure 1.

CONCLUSION

By using synchrotron X-ray powder diffraction technique, we succeed to determine a structural model for the heterobimetallic $[\text{Cu}_2\text{Mn}_2(\text{bopba})(\text{DMSO})_7]\text{DMSO}$ (**1a**) compound. The magnetic properties were investigated and thanks to the knowledge of the structure, it was possible to model intrachain magnetic interaction. It was also shown that the desolvation of **1a** leads to a loss of crystallinity and long magnetic order.

ACKNOWLEDGMENTS.

The authors would like to acknowledge financial support from CAPES, CNPq and FAPERJ. We also acknowledge the LNLS (Laboratório Nacional de Luz Síncrotron) for use of the D10B beam line. M.A. thanks CNPq for a fellowship that enabled his work that was carried as a visiting professor at Universidade Federal Fluminense. We thank Dr. Anderson Araujo Rocha for performing metal analyses and Núcleo de Estudos em Biomassa e Gerenciamento de Água (NAB) for use of laboratory facilities.

NOTES AND REFERENCES

1. O. Kahn, *Adv. Inorg. Chem.* 1995, **43**, 179.
2. O. Kahn, in *Molecular Magnetism*, VCH, New York, 1993.
3. Y. Pei, Y. Journaux and O. Kahn, *Inorg. Chem.* 1988, **27**, 399.
4. Y. Pei, M. Verdaguer, O. Kahn, J. Sletten and J. P. Renard, *Inorg. Chem.* 1987, **26**, 138.
5. O. Kahn, Y. Pei, M. Verdaguer, J. P. Renard and J. Sletten, *J. Am. Chem. Soc.*, 1988, **110**, 782.
6. K. R. Dunbar and R. A. Heintz, *Progr. Inorg. Chem.*, 1997, **45**, 283.
7. M. Verdaguer, A. Bleuzen, V. Marvaud, J. Vaissermann, M. Seuleiman, C. Desplanches, A. Sculler, C. Train, R. Garde, G. Gelly, C. Lomenech, I. Rosenman, P. Veillet, C. Cartier and F. Villain, *Coord. Chem. Rev.* 1999, **190-192**, 1023
8. M. Ohba and H. Ōkawa, *Coord. Chem. Rev.* 2000, **198**, 313.
9. J. Černák, M. Orendáč, I. Potočňák, J. Chomič, A. Orendáčová, J. Skoršep and A. Feher, *Coord. Chem. Rev.* 2002, **224**, 51.
10. P. Przychodzeń, T. Korzeniak, R. Podgajny and B. Sieklucka, *Coord. Chem. Rev.* 2006, **250**, 2234.
11. M. Shatruk, C. Avendano and K. R. Dunbar, *Progr. Inorg. Chem.* 2009, **56**, 155.
12. R. Lescouëzec, L. M. Toma, J. Vaissermann, M. Verdaguer, F. S. Delgado, C. Ruiz-Pérez, F. Lloret and M. Julve, *Coord. Chem. Rev.* 2005, **249**, 2691.
13. H. Tamaki, Z. J. Zhong, N. Matsumoto, S. Kida, M. Koikawa, N. Achiwa, Y. Hashimoto and H. Okawa, *J. Am. Chem. Soc.* 1992, **114**, 6974.
14. L. O. Atovmyan, G. V. Shilov, R. N. Lyubovskaya, E. I. Zhilyaeva, N. S. Ovanesyan, S. I. Pirumova, I. G. Gusakovskaya and Y. G. Morozov, *JETP Lett.* 1993, **58**, 766.
15. S. Decurtins, H. W. Schmalle, H. R. Oswald, A. Linden, J. Ensling, P. Gülich and A. Hauser, *Inorg. Chim. Acta* 1994, **216**, 65.
16. S. Decurtins, M. Gross, H. W. Schmalle and S. Ferlay, *Inorg. Chem.* 1998, **37**, 2443.

17. E. Coronado, J. R. Galán-Mascarós, C. J. Gómez-García and V. Laukhin, *Nature* 2000, **408**, 447.
18. M. Gruselle, M. Thouvenot, B. Malézieux, C. Train, P. Gredin, T. V. Demeschik, L. L. Troitskaya, and V. I. Sokolov, *Chem. Eur. J.* 2004, **10**, 4763.
19. C. Train, R. Gheorghe, V. Krstic, L. M. Chamoreau, N. S. Ovanesyan, G. L. J. A. Rikken, M. Gruselle and M. Verdaguer, *Nat. Mater.* 2008, **7**, 729.
20. G. Marinescu, M. Andruh, F. Lloret, and M. Julve, *Coord. Chem. Rev.* 2011, **255**, 161.
21. M. Mousavi, V. Bereau, C. Duhayon, P. Guionneau and J-P. Sutter, *Chem. Commun.* 2012, **48**, 10028.
22. E. Pardo, R. Ruiz-García, J. Cano, X. Ottenwaelde, R. Lescouëzec, Y. Journaux, F. Lloret, M. Julve, *Dalton Trans.* 2008, 2780.
23. H. O. Stumpf, L. Ouahab, Y. Pei, D. Grandjean and O. Kahn, *Science* 1993, **261**, 447.
24. M. G. F. Vaz, L. M. M. Pinheiro, H. O. Stumpf, A. F. C. Alcañtara, S. Golhen, L. Ouahab, O. Cador, C. Mathoniere and O. Kahn, *Chem. Eur. J.* 1999, **5**, 1486.
25. O. Cador, M. G. F. Vaz, C. Mathoniere and H. O. Stumpf, *J. Magn. Magn. Mater.* 2001, **234**, 6.
26. O. Cador, M. G. F. Vaz, H. O. Stumpf, C. Mathonière and O.Kahn, *Synth. Met.*, 2001, **122**, 559.
27. C. L. M. Pereira, E. F. Pedroso, H. O. Stumpf, M. A. Novak, L. Ricard, R. Ruiz-Garcia, E. Rivière and Y. Journaux, *Angew. Chem. Int. Ed.*, 2004, **43**, 956.
28. M-C. Dul, E. Pardo, R. Lescouëzec, Y. Journaux, J. Ferrando-Soria, R. Ruiz-García, J. Cano, M. Julve, F. Lloret, D. Cangussu, C. L. M. Pereira, H. O. Stumpf, J. Pasán and C. Ruiz-Pérez, *Coord. Chem. Rev.* 2010, **254**, 2281.
29. R. A. A. Cassaro, S. Ciattini, S. Soriano, H. S. Amorim, N. L. Speziali, M. Andruh and M. G. F. Vaz, *Cryst. Growth Des.* 2013, **13**, 2711.
30. J. Ferrando-Soria, M. Castellano, R. Ruiz-García, J. Cano, M. Julve, F. Lloret, C. Ruiz-Pérez, J. Pasán, L. Cañadillas-Delgado, D. Armentano, Y. Journaux and E. Pardo, *Chem. Eur. J.* 2013, **19**, 12124.

31. E. Pardo, C. Train, R. Lescouëzec, Y. Journaux, J. Pasán, C. Ruiz-Pérez, F. S. Delgado, R. Ruiz-García, F. Lloret and C. Paulsen, *Chem. Commun.* 2010, **46**, 2322.
32. A discussion of methods and examples of structure determination from powder diffraction can be found: W. I. F. David, K. Shankland, L. B. McCusker and C. Baerlocher, in *Structure Determination from Powder Diffraction Data*, Oxford University Press, 2006.
33. M. Kalisz, M. A. Novak, C. B. Pinheiro, A. S. Florencio, G. Chapuis, A. Caneschi and M. G. F. Vaz, *J. Braz. Chem. Soc.* 2007, **18**, 916.
34. H. O. Stumpf, Y. Pei, O. Kahn, J. Sletten and J. P. Renard, *J. Am. Chem. Soc.* 1993, **115**, 6738.
35. Y. Pei, J. Sletten and O. Kahn, *J. Am. Chem. Soc.* 1986, **108**, 3143.
36. J. Seiden, *J. Phys. Lett. (Paris)*, 1983, **44**, L-947.
37. M. Kalisz, M. A. Novak, H. S. Amorim, J. P. Sinnecker, and M. G. F. Vaz, *J. Magn. Magn. Mat.*, 2005, **294**, e51.
38. E. Pardo, R. Ruiz-García, F. Lloret, J. Faus, M. Julve, Y. Journaux, M. A. Novak, F. S. Delgado and C. Ruiz-Pérez. *Chem. Eur. J.* 2007, **13**, 2054.
39. M. G. F. Vaz, E. Pedroso, N. L. Speziali, M. A. Novak, A. F. C. Alcantara, and H. O. Stumpf, *Inorg. Chim. Acta*, 2001, **326**, 65.
40. D. Taupin, *J. Appl. Cryst.* 1973, **6**, 380.
41. A. Boultif and D. Louer, *J. Appl. Cryst.* 2004, **37**, 724.
42. P. M. De Wolf *J. Appl. Crystallogr.* 1968, **1**, 108.
43. A. Le Bail, H. Duroy and J. L. Fourquet, *Mater. Res. Bull.* 1988, **23**, 447.
44. W. I. F. David, K. Shankland and N. Shankland, *Chem. Commun.* 1998, 931.
45. Y. G. Andreev and P. G. Bruce, *J. Chem. Soc. Dalton Trans.* 1998, 4071.
46. V. Favre-Nicolin, and R. Cerny, *J. Appl. Cryst.* 2002, **35**, 734.
47. W. I. F. David, K. Shankland, J. van de Streek, E. Pidcock, W. D. S. Motherwell, and J. C. Cole, *J. Appl. Cryst.* 2006, **39**, 910.
48. J. Rodriguez-Carvajal, in *Fullprof: a program for Rietveld Refinement and pattern matching analysis*, abstract of the Satellite Meeting on Powder Diffraction of the XV Congress of IUCr, Toulouse, France, 1990, 127.

Table 1. Crystal data and cell parameter obtained by Rietveld refinement for **1a**.

Chemical formula	C ₃₆ H ₅₄ N ₄ O ₂₀ S ₈ Cu ₂ Mn ₂
Fw (g mol ⁻¹)	1356.38
Cell setting	Monoclinic
Space group	P2 ₁ /c
Temperature (K)	300
a, b, c (Å)	16.915(1), 9.133(1), 18.184(2)
α, β, γ(°)	90, 92.98(1), 90
V (Å ³)	2805.3(5)
Z	2
Z'	½
R _p (%)	14.5
R _{wp} (%)	14.8
R _{exp} (%)	9.01
χ ²	2.71
CCDC	1416397

CAPTION TO THE FIGURES

Figure 1 – Diffraction pattern of **1a**. The continuous line is the fitted diffractogram from the Rietveld method (as implemented in the Fullprof program), and dots represents the experimental data.

Figure 2. The connectivity mode of $\{\text{Cu}_2(\text{bopba})\}^{4-}$ ligands with the manganese ions for **1a**. Color code: green: copper; pink: manganese; grey: carbon; red: oxygen; blue: nitrogen; yellow: sulfur. Hydrogen atoms were omitted for clarity.

Figure 3. The topology of the 2-D coordination polymer (views a and b) for **1a**. The binuclear copper building block, $\{\text{Cu}_2(\text{bopba})\}$, is represented as orange rods; the oxamato-bridged Cu-Mn fragments are represented as black rods.

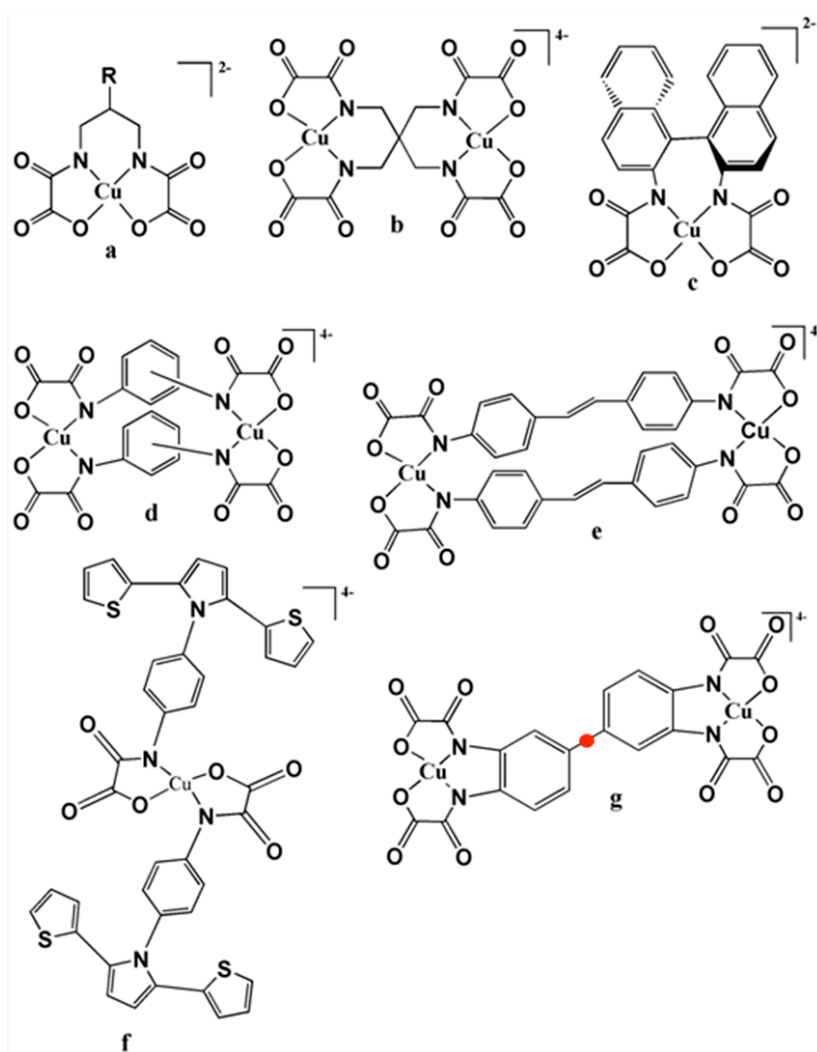
Figure 4. Views of the coordination polymer (**1a**) along the crystallographic axis *a*. The schematic representation from Figure 3 is incorporated. Hydrogen atoms were omitted for clarity.

Figure 5. Packing diagram showing parallel layers and the DMSO molecules between them for **1a**. Hydrogen atoms were omitted for clarity. The schematic representation from Figure 3 is incorporated.

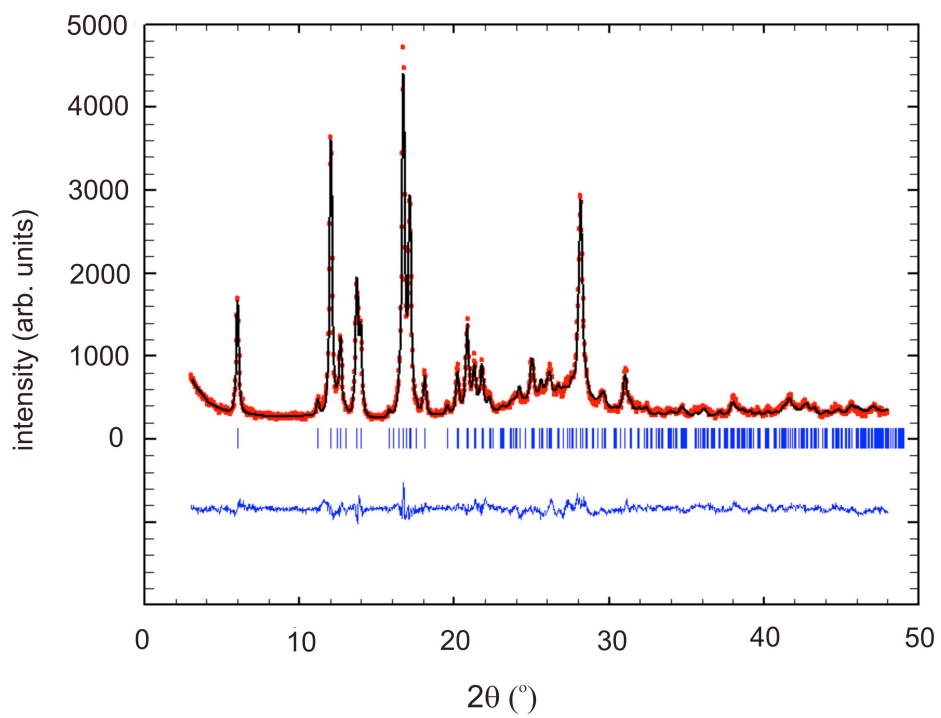
Figure 6. The temperature dependence of the $\chi_M T$ product for **1a** at 1000 Oe. The black solid line is a fit as described in the text to the data for $T > 70\text{K}$. Inset: Zoom at high temperature range.

Figure 7. Temperature dependence of $\chi_M T$ for **1a** (empty circles) and for **1b** (full circles) at 10 Oe.

Chart 1:



The red dot at **g** represents the inversion center of the molecule.

**Figura 1**

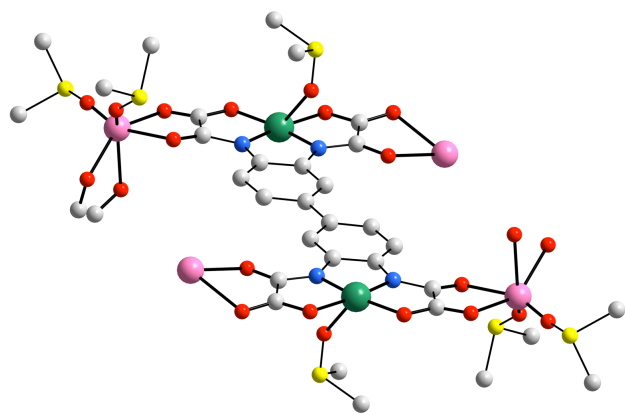
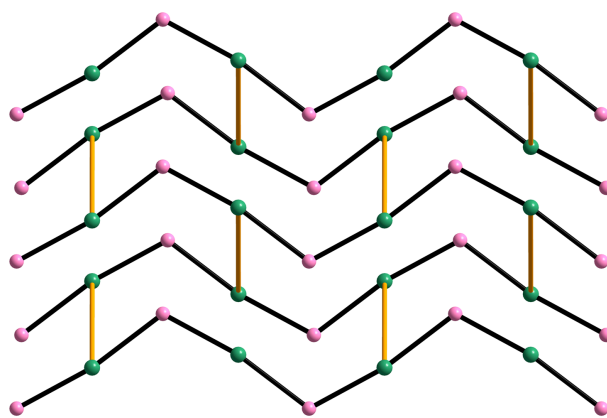
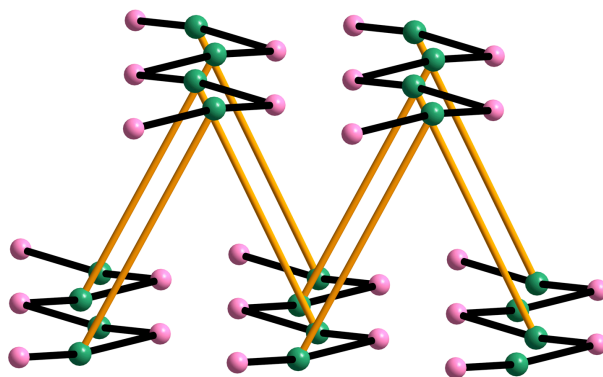


Figure 2



a



b

Figure 3

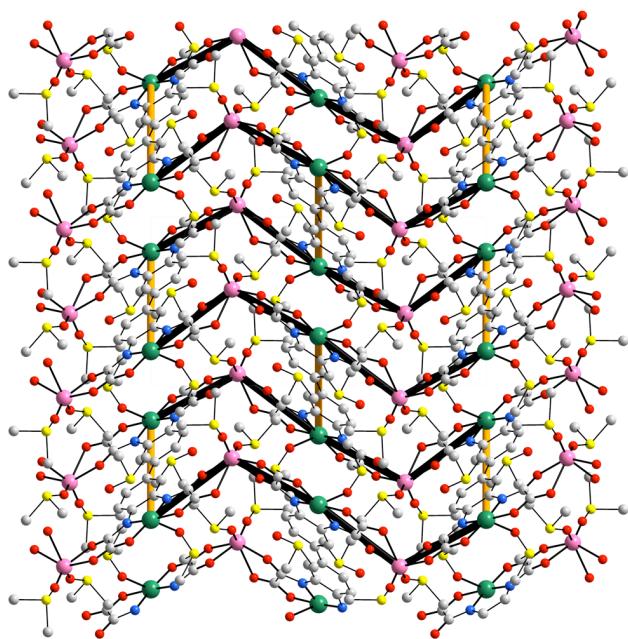


Figure 4

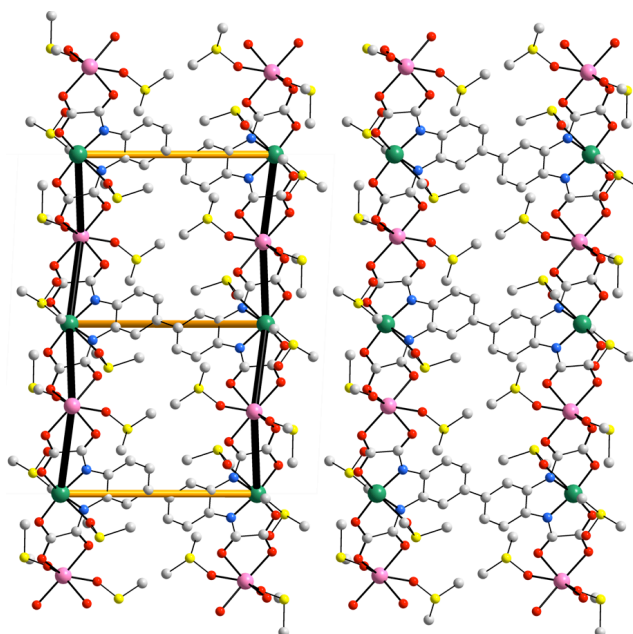
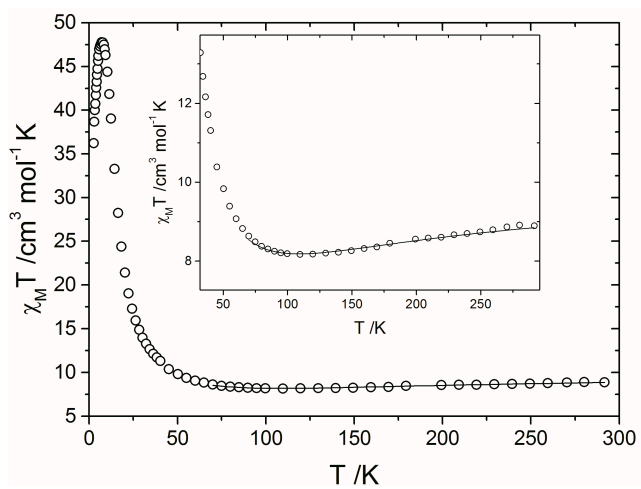
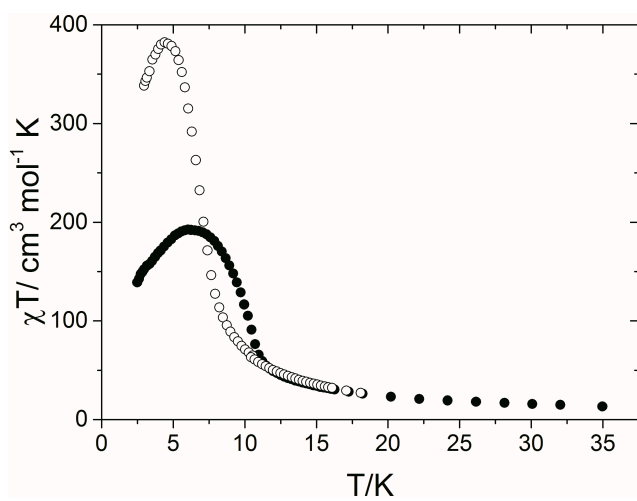


Figure 5

**Figure 6****Figure 7:**

Insert Table of Contents artwork here

The structure of a magnetic two-dimensional $\text{Cu}^{\text{II}}\text{-Mn}^{\text{II}}$ heterometallic coordination polymer was solved by using synchrotron X-ray powder diffraction

